Conversion of Protein Farnesyltransferase to a Geranylgeranyltransferase†

Kimberly L. Terry,‡ Patrick J. Casey,§ and Lorena S. Beese*,‡

Department of Biochemistry and Department of Pharmacology and Cancer Biology, Duke University Medical Center, Durham, North Carolina 27710

Received February 10, 2006; Revised Manuscript Received May 31, 2006

ABSTRACT: Posttranslational modifications are essential for the proper function of a number of proteins in the cell. One such modification, the covalent attachment of a single isoprenoid lipid (prenylation), is carried out by the CaaX prenyltransferases, protein farnesyltransferase (FTase) and protein geranylgeranyltransferase type-I (GGTase-I). Substrate proteins of these two enzymes are involved in a variety of cellular functions but are largely associated with signal transduction. These modified proteins include members of the Ras superfamily, heterotrimeric G-proteins, centromeric proteins, and a number of proteins involved in nuclear integrity. Although FTase and GGTase-I are highly homologous, they are quite selective for their substrates, particularly for their isoprenoid diphosphate substrates, FPP and GGPP, respectively. Here, we present both crystallographic and kinetic analyses of mutants designed to explore this isoprenoid specificity and demonstrate that this specificity is dependent upon two enzyme residues in the β subunits of the enzymes, W102β and Y365β in FTase (T49β and F324β, respectively, in GGTase-I).

Proteins are an essential component of cellular membranes, and may be associated with the membrane in a variety of ways (*1*, *2*). These membrane interactions include the direct insertion of a portion of the protein sequence or of some form of lipid-based moiety covalently attached to the protein (integral membrane proteins) or the noncovalent association with anchored proteins or the membrane itself (peripheral membrane proteins). The class of lipidated proteins contains lipids of varying length and complexity. In eukaryotes, one subset of lipidated proteins is posttranslationally modified by the covalent addition of an isoprenoid lipid near their *C*-terminus (*3*).

There are three known protein prenyltransferases in eukaryotic cells: protein farnesyltransferase (FTase[1]) and protein geranylgeranyltransferase type I (GGTase-I), collectively termed CaaX prenyl-transferases and geranylgeranyltransferase type II (GGTase-II or Rab GGTase), whose substrates are limited to members of the Rab subfamily of G-proteins (*4*). FTase and GGTase-I transfer either a 15- or 20-carbon isoprenoid (donated by farnesyl diphosphate, FPP, or geranylgeranyl diphosphate, GGPP), respectively, to the cysteine of a *C*-terminal Ca_1a_2X motif of substrate proteins (Figure 1A). This motif, the minimum sequence necessary for catalysis (*5*), is characterized by an invariant cysteine in the fourth position from the *C*-terminus, followed by two generally small aliphatic residues and a *C*-terminal residue that determines specificity (X). The structural determinants of CaaX specificity is explored in ref 6 (*6*). Substrate proteins include members of the Ras superfamily of GTPases, several protein kinases and phosphatases, and a variety of proteins involved in nuclear integrity and centromere function (*6*, *7*).

In addition to attachment of the isoprenoid, most CaaX proteins undergo two subsequent prenylation-dependent processing steps: the proteolytic removal of the a_1a_2X tripeptide by the CaaX protease Rce1 and the carboxymethylation of the now *C*-terminal prenylcysteine residue by the methyltransferase Icmt (*8*). Rce1 and Icmt are membrane-bound proteins localized to the endoplasmic reticulum. The net result of this series of modifications is a protein that exhibits a high affinity for cellular membranes and possesses a unique structure at its *C*-terminus that can serve as a specific recognition motif in certain protein−protein interactions (*9*−*11*).

The CaaX prenyltransferases are generally highly selective for their cognate isoprenoid diphosphate substrate (*12*, *13*). The 20-carbon GGPP binds to FTase with nanomolar affinity (but as a competitive inhibitor), while the 15-carbon FPP is a poor substrate for GGTase-I. Crystal structures of FTase in complexes with FPP and FPP analogues (*6*, *14*−*21*) show that the 15-carbon binds along one side of the active site, with the diphosphate bound in a positively charged cleft near the top of the pocket and the lipid tail extending down into the pocket. Crystal structures of GGTase-I in complex with GGPP or GGPP analogues (*6*, *20*, *22*) demonstrate that the longer isoprenoid also binds along one side of the active site of the enzyme with the diphosphate moiety, binding in a positively charged cleft near the subunit interface and the isoprenoid extending into the hydrophobic pocket. Both GGPP and GGPP analogues adopt an unusual binding conformation in GGTase-I: the first three isoprene units bind in an extended conformation along one side of the active site in a manner similar to that of FPP in the FTase active site, but the fourth isoprene unit sits at a 90° angle relative to the rest of the lipid molecule, across the bottom of the active site.

† This work was supported by grants from the NIH to L.S.B. (GM52382) and P.J.C. (GM46372).

* To whom correspondence should be addressed. Tel: (919) 681-5267. Fax: (919) 684-8885. E-mail: lsb@biochem.duke.edu.

‡ Department of Biochemistry.

§ Department of Pharmacology and Cancer Biology.

[1] Abbreviations: FPP, farnesyl diphosphate; FTase, protein farnesyltransferase; GGTase-I, protein geranylgeranyltransferase type-I.; GGPP, geranylgeranyl diphosphate; G protein, GTP binding protein; rmsd., root-mean-square deviation; PDB ID, Protein Data Bank identifier.

10.1021/bi060295e CCC: $33.50
Published on Web 07/25/2006

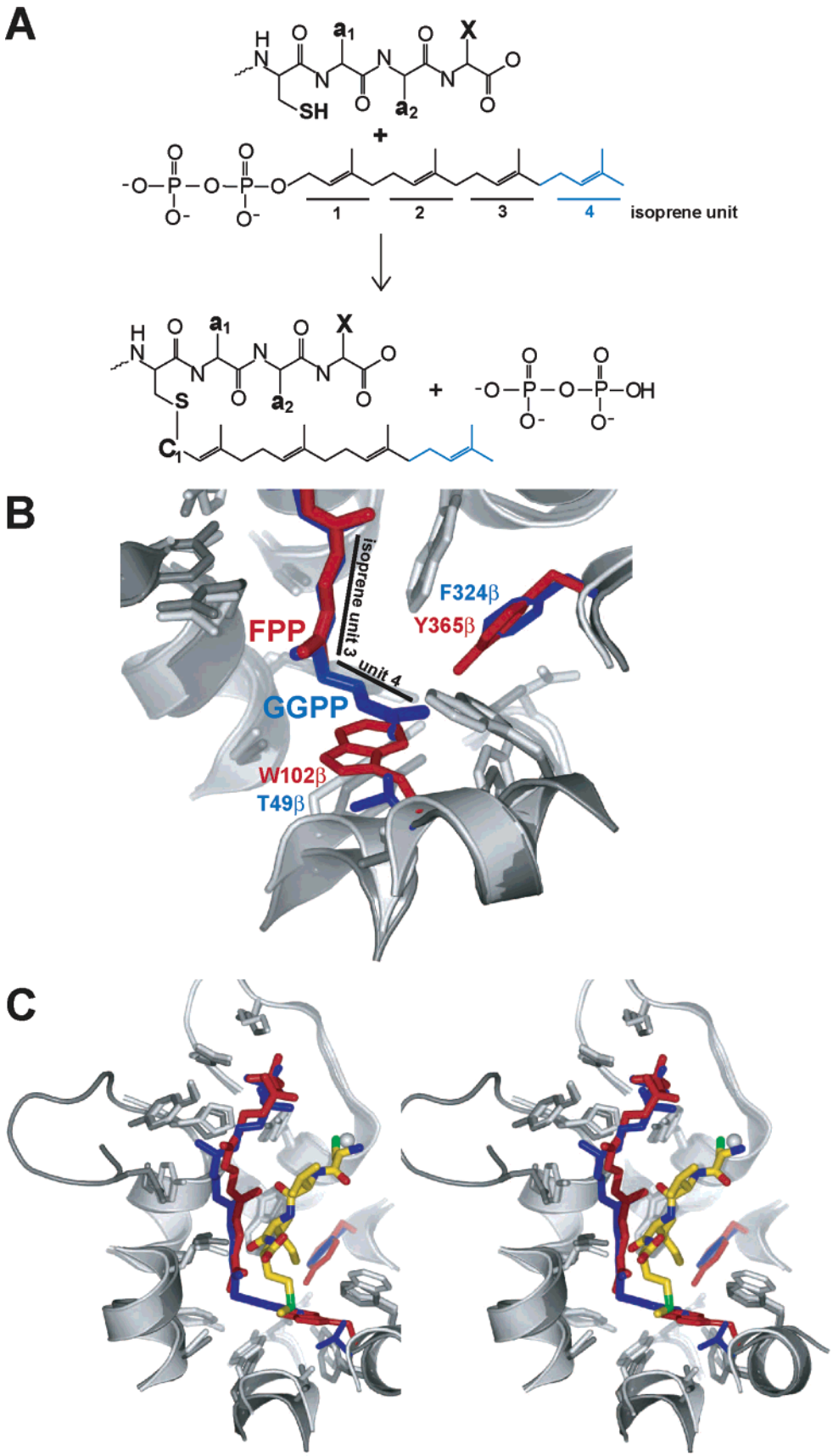

FIGURE 1: (A) Diagram of CaaX prenylation reaction. In this reaction, a thioether bond is formed between the C1 atom of the isoprenoid and the CaaX cysteine sulfur. (B) Superposition of FTase (light gray) and GGTase-I (dark gray), illustrating the binding of FPP (red) and GGPP (blue) in their respective active sites (Protein Data Bank identifiers (PDB IDs) 1S63 and 1N4P, respectively). This comparison highlights two residues (FTase: W102β and Y365β (red); GGTase-I: T49β and F324β (blue)) that are key determinants of isoprenoid diphosphate specificity. (C) Stereo diagram of the FTase and GGTase-I active sites (light gray and dark gray, respectively) (in a slightly different orientation from that in (B) for clarity), showing an FTase CaaX peptide substrate (yellow) (PDB ID 1D8D) demonstrates the extensive contact between the isoprenoid diphosphate (FPP in red, GGPP in blue) and CaaX substrates.

FTase and GGTase-I share a common α subunit, but differ in their β subunit, which determines isoprenoid diphosphate substrate selectivity. Superposition of FTase and GGTase-I illustrates the similarities and differences in their isoprenoid binding sites (Figure 1B). The binding site for the first three isoprene units of the lipid is essentially the same in FTase and GGTase-I. Two highly conserved GGTase-I residues in contact the fourth GGPP isoprene unit differ significantly in the corresponding region in FTase. The placement of the observed binding conformation of the fourth isoprene unit of GGPP in GGTase-I in the corresponding region in FTase leads to a steric clash with W102β and Y365β (T49β and F324β, respectively, in GGTase-I), suggesting that one or both of these residues may be key determinants of isoprenoid specificity (*22*).

The determinants for isoprenoid diphosphate specificity are further complicated by the observation that the CaaX moiety of the protein (or peptide) substrate is also in van der Waals contact with the isoprenoid diphosphate substrate, forming a significant portion of the isoprenoid binding site (Figure 1C). Contact between the two substrates occurs primarily between the third and fourth isoprene units of the isoprenoid and the a_2 and X residues of the CaaX substrate. This contact, particularly with the *C*-terminal specificity-determining amino acid of the CaaX substrate, introduces the possibility of cooperative substrate specificity in the CaaX prenyltransferases.

The construction of an FTase that geranylgeranylates FTase CaaX substrates or a GGTase that farnesylates its CaaX substrates could be quite useful because this technique could allow one to determine the in vivo effects of alternate prenylation on cellular localization and function. To enable this process, we have re-engineered FTase through site-directed mutagenesis in an effort to create an FTase capable of geranylgeranylating its native CaaX substrates. Here, we present the development and characterization of these re-engineered enzymes by crystallographic and kinetic methods. The results of these experiments indicate that two residues (W102β/T49β and Y365β/F324β in FTase/GGTase-I) are primary determinants of isoprenoid diphosphate selectivity in the CaaX prenyltransferases. The single mutant W102T in FTase can act as a molecular switch in the process of isoprenoid selectivity.

EXPERIMENTAL PROCEDURES

Protein Mutagenesis. Mutagenesis of the human FTase sequence in the pT5T plasmid (with the sequence for both subunits of the enzyme expressed as a translationally coupled operon, with a microtubule epitope Glu-Glu-Phe on the *C*-terminus of the α-subunit to facilitate purification (*16*)) was performed using the QuikChange site-directed mutagenesis system (Stratagene), as previously described for the W102T mutant (*22*). The mutation of the Y365β residue against a background of wild-type FTase resulted in a single mutant converting the Y365β residue to a Phe (Y365F mutant). This mutation in a background of the W102T mutant produced the double mutant W102T/Y365F. Each of these mutations was confirmed by a sequencing of the entire gene.

Protein Expression, Purification, and Crystallization. Human (wild-type and mutant) FTase and GGTase-I were expressed and purified as previously described (*15*, *16*). The W102T FTase protein used for crystallization was purified in the presence of GGPP, as described for the purification of GGTase-I (*22*). Product complexes of human FTase (both wild-type and mutant forms) were formed prior to crystallization by incubation first with an isoprenoid diphosphate substrate (FPP or GGPP; Sigma), followed by a peptide, a chimera derived from the *C*-terminus of Rap2a and the CaaX motif of H-Ras (DDPTASA**CVLS**, Genosys, >95% purity), for a final FTase−isoprenoid−CaaX molar ratio of 1:2:3, as described previously (*17*). These complexes were crystallized, cryoprotected, and flash-cooled in liquid nitrogen as previously described (*15*, *16*).

Crystallographic Data Collection, Model Building, and Refinement. Diffraction data were collected at 100 K with R-Axis II and R-Axis IV image plate systems (Molecular Structure Corporation) mounted on a Rigaku RU-200 rotating anode generator with double mirror optics (MSC). Diffraction data were also collected at the X25 beamline at the National Synchrotron Light Source, Brookhaven National Laboratories (BNL-NSLS) and at the SER-CAT beamline at the Advanced Photon Source, Argonne National Laboratories (ANL-APS). Data were integrated and scaled using HKL2000 (*23*) and XDS (*24*). The phases were determined by molecular replacement using CNS v1.0 (*25*). The structures were refined by iterative cycles of model building in O (*26*), followed by minimization and B-factor refinement using CNS v1.0. MolProbity (*27*) was used to detect steric clashes, uncommon rotamers, and Ramachandran plot outliers within the structures. All water molecules included in the final model have at least a 3σ peak in F_o-F_c maps, with density recapitulated in $2F_o-F_c$ maps. Data collection and refinement statistics are summarized in Table 1. The superpositions utilized all homologous Cα atoms in the enzymes, as performed using Swiss PDB Viewer (*28*). The rmsd differences were calculated using these structure-based superpositions of the entire protein. PYMOL (*29*) was used to create all figures.

Specific Activity Determinations. Specific activity determinations of WT and mutant CaaX prenyltransferases were conducted as previously described (*22*). Reaction mixtures containing 50 ng of either FTase (wild-type or mutant) or GGTase-I, 500 nM [^{3}H]FPP or [^{3}H]GGPP, and 1 μM Ras-CVLS (wild-type H-Ras; a cognate FTase CaaX substrate) or Ras-CVLL (H-Ras with a single mutation in the CaaX sequence (CVL***S*** to CVL***L***) to produce a GGTase-I CaaX substrate) were incubated at 30 °C for 10 min. The reactions were quenched with SDS, and the protein was precipitated by TCA. The samples were glass-fiber filtered and trapped radiolabeled isoprenoid detected by scintillation counting.

Steady-State Rate Constant Determinations. Steady-state kinetic determinations were conducted using the same assay as that described above but with modifications to allow accurate kinetic parameters to be obtained even with low substrate concentrations. All reactions contained 25 ng of enzyme and increased detergent levels to keep the isoprenoid diphosphate substrates in solution (0.2% β-octylglucoside (OG) in all reactions with FPP and 5 mM Zwittergent 3−14 in all reactions with GGPP; all reactions contained 1 mM EDTA). Isoprenoid utilization was determined in assays in which isoprenoid diphosphate concentrations were varied from 5 to 320 nM at a protein substrate concentration of 1.5 μM. Protein substrate utilization was determined in assays

Table 1: Crystallographic Data Collection and Refinement Statistics

complex	WT FTase farnesyl-CVLS	W102T geranylgeranyl-CVLS	Y365F farnesyl-CVLS	W102T/Y365F geranylgeranyl-CVLS
Data Collection (All Data)	ANL-APS SER−CAT	Cu Kα[d]	BNL-NSLS ×25	Cu Kα[d]
resolution, Å	50−1.5 (1.55−1.50)	50−1.85 (1.92−1.85)	50−1.80 (1.86−1.80)	50−3.00 (3.18−3.00)
no. reflections: unique/total	184,708/1,319,500	98,678/372,133	109,005/1,005,969	21,656/100,685
mean I/σ_1[c]	25.2 (2.5)	16.2 (1.9)	25.5 (6.5)	9.92 (2.88)
R_{sym} %[a]	6.4 (64.2)	7.1 (48.4)	8.9 (51.6)	15.4 (38.5)
unit cell				
$a = b$ (Å)	178.6	178.5	178.8	178.6
c (Å)	64.7	64.6	64.6	65.1
Refinement ($F \geq 0\sigma$)				
completeness (%)	98.3 (90.8)	98.2 (97.0)	99.8 (97.9)	89.9 (88.2)
R_{cryst}[b] (%)	19.0 (27.8)	18.7 (29.3)	17.7 (20.2)	26.8 (37.8)
R_{free}[b] (%)	20.3 (27.8)	20.7 (30.5)	18.0 (22.3)	27.8 (37.5)
nonhydrogen atoms: total/H_2O	6,704/716	6,612/634	6,722/708	6,021/44
rmsd from ideal geometry				
bond lengths (Å)	0.004	0.005	0.005	0.011
bond angles (deg)	1.16	1.16	1.16	1.40
average isotropic B value (Å^2)	18.9	23.8	20.4	38.2
sigmaA coordinate error (Å^2)	0.12	0.19	0.11	0.70
MolProbity analysis				
all-atom clash score	7.0	7.7	6.9	13.9
rotamer analysis[e,f]	0.16 (1/643)	0.16 (1/643)	0.15 (1/646)	0.16 (1/643)
Ramachandran: favored (%)	97.7	97.6	97.7	96.7
allowed (%)	100.0	100.0	100.0	100.0
PDB ID	2H6F	2H6G	2H6H	2H6I

[a] $R_{sym} = (\Sigma|(I - \langle I \rangle)|)/(\Sigma I)$, where $\langle I \rangle$ is the average intensity of multiple measurements. [b] R_{cryst} and $R_{free} = (\Sigma|F_{obs} - F_{calc}|)/(\Sigma|F_{obs}|)$. R_{free} was calculated over 5% of the amplitudes not used in refinement. [c] Values in parentheses correspond to those in the outer resolution shell. [d] Rigaku RU-H3R rotating anode generator. [e] Percentage of rotamers observed in <1% of structures in rotamer library. [f] Number of rotamers observed in <1% of structures in rotamer library/total number of residues in model.

in which the isoprenoid diphosphate concentration was held at 250 nM and protein substrate concentrations varied from 0.1 to 4.6 μM. The reactions were carried out at 30 °C for 5 min, quenched, precipitated, filtered, and counted as described above. A weighted double-reciprocal plot of the turnover rates versus substrate concentration, employing Microsoft Excel software, was used to determine the K_M and V_{max} values for each substrate combination, from which the k_{cat} and k_{cat}/K_M values were calculated.

RESULTS

Structure of Wild-Type FTase. To study the effects of the W102β and Y365β mutations in FTase, we determined the crystal structures of the mutants in complexes that represent key steps in the reaction cycle. The substrate peptide employed in these structural studies was a chimera derived from the sequences of Rap2a (the sequence just *N*-terminal to the CaaX motif: DDPTASA) and H-Ras (the CaaX motif: CVLS). Intact H-Ras was used as the native FTase CaaX substrate in the kinetic assays detailed below.

We determined the structure of wild-type human FTase in a complex with the farnesylated product of the chimeric peptide. The structure of the enzyme in this complex was essentially identical to previously determined structures of human FTase (*6*, *16*, *18*−*20*). Superposition of the enzyme in this complex with that of the previously determined FTase structure with a farnesylated K-Ras4B peptide product (*17*) shows that the farnesylated product of both complexes bind in a homologous manner (Figure 2A). Superposition of this structure with that of FTase in a substrate ternary complex with an FPP analogue and an H-Ras-derived peptide (*6*) shows the similarity of binding of the CaaX motif of the farnesylated peptide product and the H-Ras peptide previously observed (Figure 2B). These superpositions show an rmsd of the farnesyl moiety (all atoms; with respect to the K-Ras4B peptide product complex) of 0.34 Å and an rmsd of the CaaX motif (Cα atoms; with respect to the H-Ras peptide ternary complex) of 0.39 Å.

The resolution of this structure (1.5 Å) is significantly higher than any previously determined for either of the CaaX prenyltransferases, clarifying the coordination of the zinc ion required by these enzymes for catalysis. Previous structures of FTase (*6*, *14*−*22*, *30*−*32*) suggest a distorted pentacoordinate system around the zinc ion, including the enzyme residues D297β (bidentate interaction), C299β, and H362β and the cysteine of the CaaX peptide (in both substrate- and product-bound complexes). Recent XAFS studies (*33*), however, suggested that the zinc coordination sphere may be tetrahedral and that D297β is monodentate. In this structure, we are able to observe these interactions at the highest resolution to date, yielding a detailed model of the FTase zinc ion coordination sphere (Figure 2C). In this high resolution structure of the farnesylated peptide product, we observe unequivocally the zinc in a distorted pentacoordinate coordination geometry formed by the peptide product cysteine (albeit at a long liganding distance, 2.7Å) and the enzyme residues C299β, H362β, and the bidentate D297β.

Characterization of the W102T Single Mutant. Consistent with our previous study (*22*), initial steady-state activity assays showed that the conversion of W102β to Thr in FTase results in an enzyme capable of geranylgeranylating typical FTase substrate proteins (Figure 3, Table 2). The turnover rate for the geranylgeranylation reaction catalyzed by the W102T variant (0.41 mol·s^{-1}) is similar to that observed for the farnesylation reaction catalyzed by wild-type FTase (0.50 mol·s^{-1}). This mutation also essentially abolishes FPP

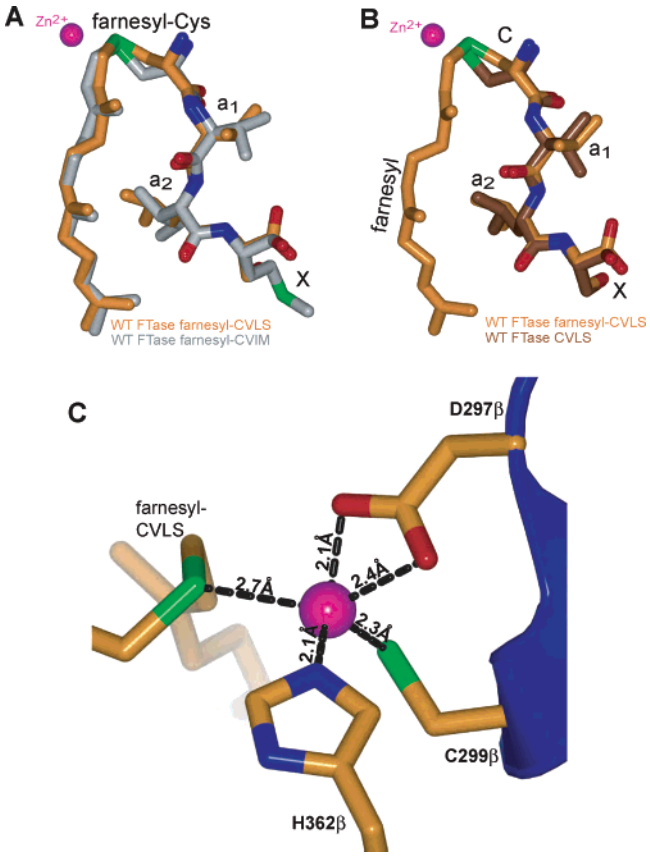

FIGURE 2: Farnesylated CaaX peptide product binding in the wild-type FTase active site. (A) Superposition of wild-type FTase in complex with the farnesyl-CVLS peptide product (yellow) and the farnesyl-CVIM peptide product (gray) (PDB ID 1KZP) (*17*) illustrates the similarity in the farnesyl-moiety binding conformations. (B) Superposition of wild-type FTase in complex with the farnesyl-CVLS peptide product (yellow) and a ternary complex with an FPP analogue (not shown, for clarity) and the CVLS peptide substrate (brown) (PDB ID 1TN8) (*6*) illustrates the similarity in the CaaX binding conformations. (C) Zinc binding site of wild-type FTase. The zinc ion (magenta) is coordinated by three enzyme residues (D297β, C299β, and H362β) and the cysteine of the farnesylated peptide product complex.

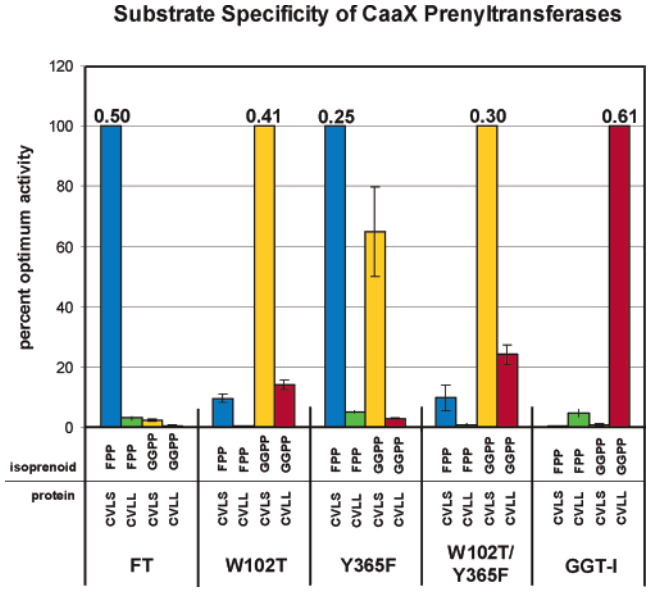

FIGURE 3: Altered substrate specificity of a protein prenyltransferase. Prenylation reactions assayed the activity of human WT FTase, WT GGTase-I, and three FTase mutants (W102T, Y365F, and W102T/Y365F) with four substrate combinations: FPP + Ras-CVLS (cognate FTase substrates (blue)), FPP + Ras-CVLL (green), GGPP + Ras-CVLS (yellow), and GGPP + Ras-CVLL (GGTase-I substrates (red)). The activities are shown as percentages of activity with optimal isoprenoid diphosphate and protein substrates for each of the enzymes tested (FPP and Ras-CVLS, FTase; GGPP and Ras-CVLS, W102T FTase; FPP and Ras-CVLS, Y365F; GGPP and Ras-CVLS, W102T/Y365F; GGPP and Ras-CVLL, GGTase-I). The turnover rates (given as moles of prenylated product per mole of enzyme per minute of reaction) are indicated for the optimal substrate combinations for each enzyme.

usage as a substrate, while still retaining specificity for typical FTase protein (peptide) substrates. The observed specificity constants (k_{cat}/K_M) for the W102T mutant ($0.48 \cdot 10^6$ $M^{-1} \cdot s^{-1}$ and $0.70 \cdot 10^4$ $M^{-1} \cdot s^{-1}$) for GGPP and the FTase substrate

Table 2: Steady-State Rate Constants for Wild-Type FTase, GGTase-I, and the W102T FTase Mutant for All Substrate Combinations with at Least 25% of the Activity of the Optimal Combination, As Shown in Figure 3[a]

				isoprenoid diphosphate substrate		CaaX substrate	
enzyme	isoprenoid diphosphate	Ras-CaaX[b]	k_{cat} (s^{-1})	K_M (nM)	k_{cat}/K_M (10^6 M^{-1} s^{-1})	K_M (μM)	k_{cat}/K_M (10^4 M^{-1} s^{-1})
WT FTase	FPP	CVLS	0.014 ± 0.001	22.16 ± 3.89	0.65 ± 0.12	0.90 ± 0.16	1.58 ± 0.06
W102T	GGPP	CVLS	0.015 ± 0.002	32.79 ± 5.25	0.48 ± 0.08	2.23 ± 0.38	0.70 ± 0.03
WT GGTase-I	GGPP	CVLL	0.021 ± 0.002	39.34 ± 14.91	0.59 ± 0.20	1.33 ± 0.34	1.64 ± 0.26

[a] Isoprenoid utilization was determined in assays in which isoprenoid diphosphate concentrations were varied from 5 to 320 nM at a protein substrate concentration of 1.5 μM; the protein substrate utilization was determined in assays in which the isoprenoid diphosphate concentration was held at 250 nM and protein substrate concentrations varied from 0.1 to 4.6 μM. A weighted double-reciprocal plot of the turnover rates versus substrate concentration was used to determine the steady-state rate constants. For simplicity, the k_{cat} value determined at a constant isoprenoid concentration is shown, and was used for k_{cat}/K_M calculations. [b] Ras-CaaX indicates H-Ras CaaX sequence: Ras-CVLS = WT FTase substrate; Ras-CVLL = WT GGTase-I substrate.

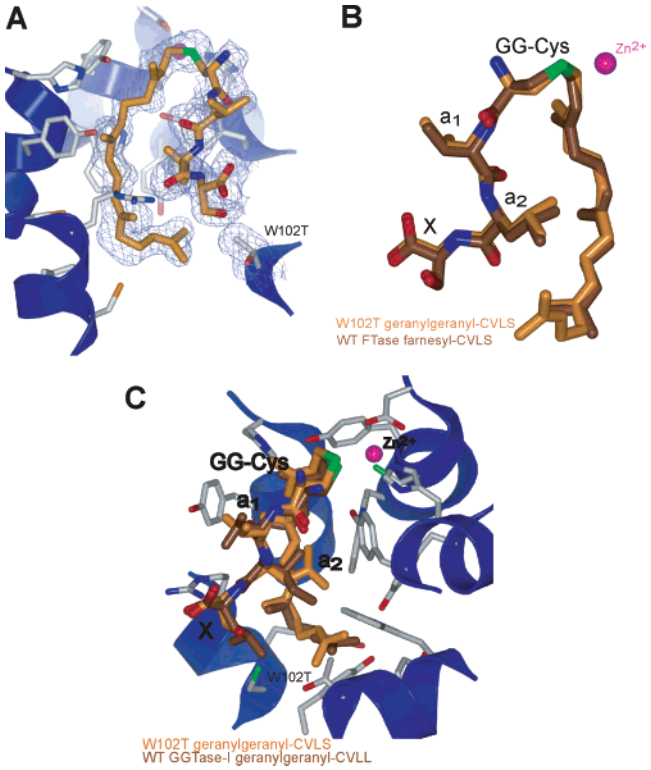

FIGURE 4: Geranylgeranylated CaaX peptide product binding in the active site of the W102T mutant. (A) Simulated-annealing omit maps (F_o-F_c, contoured at 2 σ; blue) confirm the conversion of residue W102β to Thr and indicate the binding conformation of the geranylgeranyl peptide product (yellow) in the active site of the enzyme. (B) Superposition of the W102T mutant and wild-type FTase illustrates the similar binding conformation of the geranylgeranylated peptide product (in the W102T mutant (yellow)) and the farnesylated-peptide product (in wild-type FTase (brown)). (C) Superposition of the W102T mutant and wild-type GGTase-I demonstrates the binding of the geranylgeranyl moiety of their respective peptide products (W102T, yellow; GGTase-I, brown).

protein Ras-CVLS, respectively, are similar to those determined for wild-type FTase ($0.65\cdot10^6$ $M^{-1}\cdot s^{-1}$ and $1.58\cdot10^4$ $M^{-1}\cdot s^{-1}$) and GGTase-I ($0.59\cdot10^6$ $M^{-1}\cdot s^{-1}$ and $1.64\cdot10^4$ $M^{-1}\cdot s^{-1}$) with their preferred substrates. The turnover number (k_{cat}) for the geranylgeranylation reaction in the W102T variant (0.015 s^{-1}) is similar to that of wild-type FTase farnesylating its cognate substrate Ras-CVLS (0.014 s^{-1}). Hence, this mutation switches the isoprenoid diphosphate specificity of FTase to that of GGTase-I without compromising its reaction efficiency.

To characterize the molecular basis for this switch in isoprenoid specificity, the W102T mutant was crystallized as a complex with a geranylgeranylated product of the chimeric substrate peptide described above. The structure of this complex was determined at 1.85 Å resolution. The Thr substitution is clearly visible in the electron density, as is the conformation of the bound geranylgeranylated-peptide product (Figure 4A). The mutation required a backbone shift in residues 101β−104β (approximately one helical turn), resulting in a translation of approximately 0.7 Å in residue T102β to accommodate the Thr side chain; the remainder of the enzyme was virtually identical to wild-type FTase. The conformation of the peptide portion of the product is essentially identical to that observed in the wild-type FTase complex described above, with an rmsd of 0.43 Å (all atoms) (Figure 4B). The first three isoprene units of the geranylgeranyl moiety of the product bind in a manner similar to that observed for the farnesyl group in the wild-type complex, with the additional fourth isoprene unit adopting a similar conformation to that observed in wild-type GGTase-I (*22*),

forming an approximately 90° angle to the rest of the isoprenoid (Figure 4C). There is a slight upward translation in the fourth isoprene unit in this complex, however, to accommodate the FTase Y365β residue (Phe in GGTase-I). This structure clearly demonstrates that there is ample space to accommodate the fourth isoprene unit of the geranylgeranyl group with the single substitution of Thr for W102β.

Characterization of the Y365F Single Mutant. Steady-state activity assays were also used to characterize the consequences on substrate specificity of the conversion of Y365β in FTase to a Phe (Figure 3, Table 2). These studies indicate that this mutation relaxes, rather than switches, isoprenoid diphosphate selectivity, allowing the enzyme to use either FPP or GGPP. Although this mutation decreases isoprenoid diphosphate selectivity, it does not result in significant alteration in protein substrate specificity. The conversion of Y365β to Phe in FTase does not appear to significantly affect the interaction with native isoprenoid diphosphate or CaaX substrates (FPP and Ras-CVLS, respectively) (Table 1). The turnover number of the reaction with native isoprenoid diphosphate and CaaX substrates (FPP and Ras-CVLS, respectively) for Y365F (0.007 s^{-1}) is similar to that observed for wild-type FTase (0.014 s^{-1}). This mutant also catalyzes the geranylgeranylation of the cognate FTase CaaX substrate, albeit with a significantly decreased specificity constant for the protein substrate (more than 10-fold decrease relative to that in the farnesylation reaction), possibly because of a kinked binding conformation of the GGPP molecule, which could alter the binding site of the CaaX substrate.

The structure of the Y365F mutant in complex with a farnesylated product of the substrate peptide was determined at 1.80 Å resolution. The mutation and binding conformation of the product are clearly visible in the electron density (Figure 5A). The enzyme structure is nearly identical to that of wild-type FTase; the only significant difference is the absence of the hydroxyl group on residue 365β (Phe in this mutant). The farnesylated peptide product binds in a conformation nearly indistinguishable from that in wild-type FTase, with an rmsd of 0.31 Å (all atoms) (Figure 5B). We were unable to obtain crystals of this mutant in complex with a geranylgeranylated peptide product, but it is apparent from the comparison of the isoprenoid diphosphate binding sites of FTase and GGTase-I (Figure 1B) that the Y365F mutation in FTase is not sufficient to accommodate the binding of GGPP as observed in GGTase-I. It is possible that the geranylgeranyl moiety kinks in the middle, as previously described (*31*), allowing for the accommodation of the additional five carbons of the lipid.

Characterization of the W102T/Y365F Double Mutant. The combined effect of the two mutations in FTase (W102T and Y365F) on substrate specificity was characterized by steady-state activity assays (Figure 3, Table 2). The inclusion of both mutations in a single FTase molecule results in an FTase capable of geranylgeranylating cognate FTase protein substrates. As observed with the W102T single FTase mutant, this mutant exhibits no significant utilization of FPP or alteration of CaaX substrate specificity. The geranylgeranylation of cognate FTase protein substrates by this mutant progresses with similar steady-state rate constants as that of WT FTase in its native farnesylation reaction. The combined W102T and Y365F mutations, like the W102T single

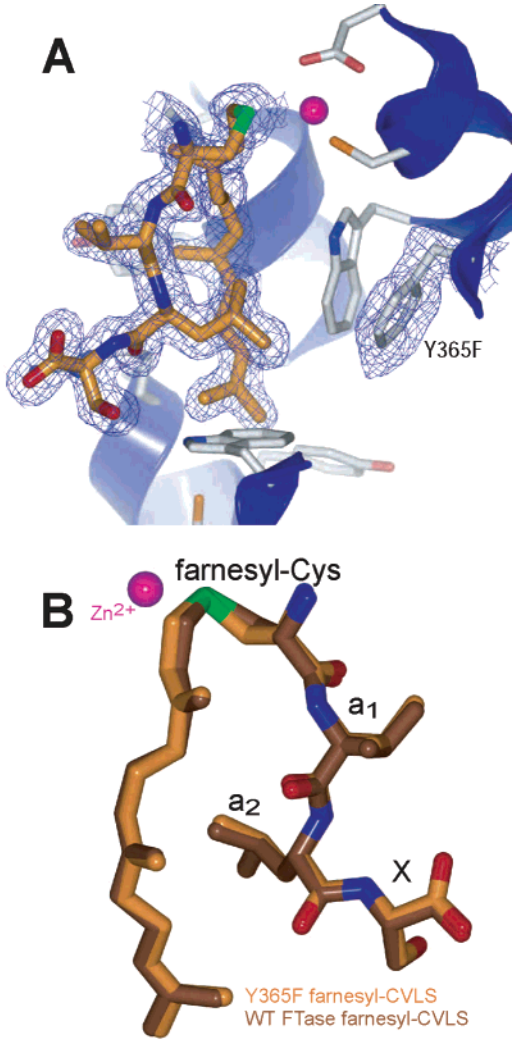

FIGURE 5: Farnesylated CaaX peptide product binding in the active site of the Y365F mutant. (A) Simulated-annealing omit maps (F_o-F_c, contoured at 4 σ; blue) confirm the conversion of residue Y365β to Phe and indicate the binding conformation of the farnesyl peptide product (yellow) in the active site of the enzyme. (B) Superposition of the Y365F mutant and wild-type FTase illustrates the comparable binding of the farnesylated peptide product in the mutant (yellow) and wild-type (brown) FTase.

mutation, switch the isoprenoid diphosphate substrate specificity of FTase without compromising catalytic efficiency.

The double mutant W102T/Y365F was crystallized in complex with a geranylgeranylated product of the chimeric substrate peptide. The structure of this complex was determined to 3.0 Å resolution. Both mutations as well as the binding conformation of the geranylgeranylated peptide product were clearly observed in the electron density (Figure 6A). As observed in the W102T mutant structure, a slight backbone shift was necessary to accommodate the T102β side chain, whereas the remainder of the protein was essentially identical to that observed in the WT FTase complexes. The peptide portion of the product adopts a similar conformation as in the WT enzyme (Figure 6B), with an rmsd of 0.47 Å (all atoms). The conformation of the geranylgeranyl moiety was similar to that observed in the W102T mutant (rmsd of 0.51 Å for all atoms; Figure 6C), with a slight shift in the fourth isoprene unit due to the absence of the hydroxyl group on the 365β residue (Phe in this mutant). This structure indicates the ability of the

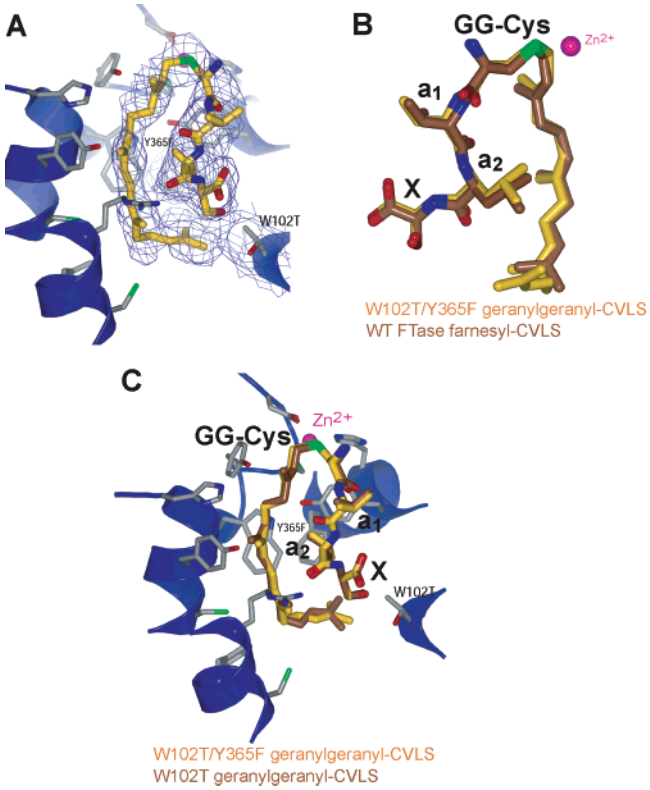

FIGURE 6: Geranylgeranylated CaaX peptide product binding in the active site of the W102T/Y365F double mutant. (A) Simulated-annealing omit maps (F_o-F_c, contoured at 3.5 σ; blue) confirm the conversion of residue W102β to Thr and residue Y365β to Phe and indicate the binding conformation of the geranylgeranyl peptide product (yellow) in the active site of the enzyme. (B) Superposition of the W102T/Y365F mutant and wild-type FTase illustrates the similar binding conformation of the geranylgeranylated peptide product (in the W102T/Y365F mutant (yellow)) and the farnesylated-peptide product (in wild-type FTase (brown)). (C) Superposition of the W102T/Y365F mutant and the W102T mutant demonstrates the binding of the geranylgeranyl moiety of their respective peptide products (W102T/Y365F, yellow; W102T, brown).

W102T/Y365F mutant to bind its isoprenoid diphosphate and CaaX substrates in wild-type conformations.

DISCUSSION

Several studies have examined the lipid specificity of isoprenoid synthase enzymes (*34*−*36*), specifically targeting product chain termination specificity. Two of these studies (*34*, *35*) employed mutagenesis to convert archaebacterial farnesyl diphosphate synthase to geranylgeranyl diphosphate synthase (and vice versa) and found a single residue of critical importance to product chain length in this family of enzymes. Here, we demonstrate that a single mutation is sufficient to interconvert the isoprenoid diphosphate specificity of FTase and GGTase-I. On the basis of crystallographic analysis, we have previously proposed two residues in the active site of the CaaX prenyltransferases to be critical in isoprenoid substrate selectivity (*22*). In that study, we presented the mutation of one of these residues (W102β in FTase to Thr, its GGTase-I counterpart) and the initial analysis of its substrate specificity. Here, we combine crystallographic and steady-state kinetic methods in the continued analysis of this and other mutants targeting the isoprenoid diphosphate specificity of the CaaX prenyltransferases.

In an effort to alter the isoprenoid diphosphate specificity of FTase, we selectively mutated W102β and Y365β to their GGTase-I counterparts (Thr and Phe, respectively), both singly and in combination. The conversion of W102β to Thr had the most dramatic effect. Kinetic analysis demonstrates that this mutant recognizes and utilizes GGPP and the cognate FTase CaaX substrate with near-wild-type efficiency. A structural analysis of the W102T mutant indicates that this mutant not only uses GGPP as a substrate but also that it does so through a binding mode similar to wild-type GGTase-I without significantly affecting the binding conformation of the CaaX substrate. The kinetic assays demonstrate that the removal of the hydroxyl group of Y365β (the Y365F mutant) relaxes isoprenoid diphosphate selectivity, allowing FTase to accept both FPP and GGPP. The removal of the hydroxyl group cannot, however, allow for the binding of the GGPP molecule in the same conformation as that observed in GGTase-I (Figure 1B); instead, GGPP may bind through a kinking along the lipid tail (*31*), altering the binding site of the CaaX substrate (Figure 1C). Consistent with this hypothesis, the specificity constant of Y365F for the cognate FTase CaaX substrate is substantially lower in the presence of GGPP versus FPP. The simultaneous conversion of W102β and Y365β in FTase has effects similar to that of the single W102T mutation, resulting in an FTase with GGTase isoprenoid diphosphate specificity.

Together, these steady-state kinetic analyses and crystallographic characterizations have demonstrated that these residues (W102β and Y365β in FTase, T49β and F324β in GGTase-I), are crucial in the selectivity of the isoprenoid diphosphate substrate in the prenyltransferases. In particular, we show that the single mutation of W102T is sufficient to switch the isoprenoid diphosphate selectivity of FTase to that of GGTase-I with near-wild-type activity, without altering

CaaX specificity. These results illustrate the simplicity of this selectivity machinery, a characteristic that might allow us to characterize the in vivo contribution of the specific prenyl modification on cellular localization and function.

ACKNOWLEDGMENT

We thank Carolyn Weinbaum and Johannes Rudolf for help with kinetic assays. We also thank the X25 (BNL-NSLS) and SER-CAT (ANL-APS) staff for their time and assistance. Data for this study were measured at the beamline X25 of the Brookhaven National Laboratory National Synchrotron Light Source (BNL-NSLS). Financial support for the Brookhaven National Laboratory comes principally from the Offices of Biological and Environmental Research and of Basic Energy Sciences of the US Department of Energy, and from the National Center for Research Resources of the National Institutes of Health. Data were also collected at Southeast Regional Collaborative Access Team (SER-CAT) 22-ID beamline at the Advanced Photon Source, Argonne National Laboratory (ANL-APS). Use of the Advanced Photon Source was supported by the US Department of Energy, Office of Science, Office of Basic Energy Sciences, under Contract No. W-31-109-Eng-38.

REFERENCES

1. Singer, S. J., and Nicolson, G. L. (1972) The fluid mosaic model of the structure of cell membranes, *Science 175*, 720−731.
2. Yeagle, P. L. (1993) *The Membranes of Cells*, 2nd ed., Academic Press, Inc., San Diego, CA.
3. Glomset, J. A., Gelb, M. H., and Farnsworth, C. C. (1990) Prenyl proteins in eucaryotic cells: a new type of membrane anchor, *Trends Biochem. Sci. 15*, 139−142.
4. Casey, P. J., and Seabra, M. C. (1996) Protein prenyltransferases, *J. Biol. Chem. 271*, 5289−5292.
5. Brown, M. S., Goldstein, J. L., Paris, K. J., Burnier, J. P., and Marsters, J. C. (1992) Tetrapeptide inhibitors of protein farnesyltransferase: amino-terminal substitutions in phenylalanine-containing tetrapeptides restores farnesylation, *Proc. Natl. Acad. Sci. U.S.A. 89*, 8313−8316.
6. Reid, T. S., Terry, K. L., Casey, P. J., and Beese, L. S. (2004) Crystallographic analysis of CaaX prenyltransferases complexed with substrates defines rules of protein substrate selectivity, *J. Mol. Biol. 343*, 417−433.
7. Spence, R. A., and Casey, P. J. (2001) in *The Enzymes* (Tamanoi, F., and Sigman, D. S., Eds.) pp 1−18, Academic Press, San Diego, CA.
8. Winter-Vann, A. M., and Casey, P. J. (2005) Post-prenylation-processing enzymes as new targets in oncogenesis, *Nat. Rev. Cancer 5*, 405−412.
9. Silvius, J. R., and l'Heureux, F. (1994) Fluorimetric evaluation of the affinities of isoprenylated peptides for lipid bilayers, *Biochemistry 33*, 3014−3022.
10. Marshall, C. J. (1993) Protein prenylation: a mediator of protein−protein interactions, *Science 259*, 1865−1866.
11. Gelb, M. H. (1997) Protein prenylation, et cetera: signal transduction in two dimensions, *Science 275*, 1750−1751.
12. Yokoyama, K., Zimmerman, K., Scholten, J., and Gelb, M. H. (1997) Differential prenyl pyrophosphate binding to mammalian protein geranylgeranyltransferase-I and protein farnesyltransferase and its consequences on the specificity of protein prenylation, *J. Biol. Chem. 272*, 3944−3952.
13. Reiss, Y., Brown, M. S., and Goldstein, J. L. (1992) Divalent cation and prenyl pyrophosphate specificities of the protein farnesyltransferase from rat brain, a zinc metalloenzyme, *J. Biol. Chem. 267*, 6403−6408.
14. Long, S. B., Casey, P. J., and Beese, L. S. (1998) Co-crystal structure of protein farnesyltransferase with a farnesyl diphosphate substrate, *Biochemistry 37*, 9612−9618.
15. Long, S. B., Casey, P. J., and Beese, L. S. (2000) The basis for K-Ras4B binding specificity to protein farnesyltransferase revealed by 2 Å resolution ternary complex structures, *Structure 8*, 209−222.
16. Long, S. B., Hancock, P. J., Kral, A. M., Hellinga, H. W., and Beese, L. S. (2001) The crystal structure of human protein farnesyltransferase reveals the basis for inhibition by CaaX tetrapeptides and their mimetics, *Proc. Natl. Acad. Sci. U.S.A. 98*, 12948−12953.
17. Long, S. B., Casey, P. J., and Beese, L. S. (2002) Reaction path of protein farnesyltransferase at atomic resolution, *Nature 419*, 645−650.
18. Reid, T. S., and Beese, L. S. (2004) Crystal structures of the anticancer clinical candidates R115777 (tipifarnib) and BMS-214662 complexed with protein farnesyltransferase suggest a mechanism of FTI selectivity, *Biochemistry 43*, 6877−6884.
19. deSolms, S. J., Ciccarone, T. M., MacTough, S. C., Shaw, A. W., Buser, C. A., Ellis-Hutchings, M., Fernandes, C., Hamilton, K. A., Huber, H. E., Kohl, N. E., Lobell, R. B., Robinson, R. G., Tsou, N. N., Walsh, E. S., Graham, S. L., Beese, L. S., and Taylor, J. S. (2003) Dual protein farnesyltransferase−geranylgeranyltransferase-I inhibitors as potential cancer chemotherapeutic agents, *J. Med. Chem. 46*, 2973−2984.
20. Reid, T. S., Long, S. B., and Beese, L. S. (2004) Crystallographic analysis reveals that anticancer clinical candidate L-778,123 inhibits protein farnesyltransferase and geranylgeranyltransferase-I by different binding modes, *Biochemistry 43*, 9000−9008.
21. Strickland, C. L., Windsor, W. T., Syto, R., Wang, L., Bond, R., Wu, Z., Schwartz, J., Le, H. V., Beese, L. S., and Weber, P. C. (1998) Crystal structure of farnesyl protein transferase complexed with a CaaX peptide and farnesyl diphosphate analogue, *Biochemistry 37*, 16601−16611.
22. Taylor, J. S., Reid, T. S., Terry, K. L., Casey, P. J., and Beese, L. S. (2003) Structure of mammalian protein geranylgeranyltransferase type-I, *EMBO J. 22*, 5963−5974.
23. Otwinowski, Z., and Minor, W. (1997) Processing of X-ray diffraction data collected in oscillation mode, *Methods Enzymol. 276*, 307−326.
24. Kabsch, W. (1993) Automatic processing of rotation diffraction data from crystals of initially unknown symmetry and cell dimensions, *J. Appl. Crystallogr. 26*, 795−800.
25. Brünger, A. T., Adams, P. D., Clore, G. M., DeLano, W. L., Gros, P., Grosse-Kunstleve, R. W., Jiang, J.-S., Kuszewski, J., Nilges, M., Pannu, N. S., Read, R. J., Rice, L. M., Simonson, T., and Warren, G. L. (1998) Crystallography & NMR System: A new software suite for marcomolecular structure determination, *Acta Crystallogr., Sect. D 54*, 905−921.
26. Jones, T. A., Zou, J. Y., Cowan, S. W., and Kjeldgaard, M. (1991) Improved methods for binding protein models in electron density maps and the location of errors in these models, *Acta Crystallogr., Sect. A 47*, 110−119.
27. Davis, I. W., Murray, L. W., Richardson, J. S., and Richardson, D. C. (2004) MOLPROBITY: structure validation and all-atom contact analysis for nucleic acids and their complexes, *Nucleic Acids Res. 32*, W615−W619.
28. Guex, N., and Peitsch, M. C. (1997) SWISS-MODEL and the Swiss-PdbViewer: an environment for comparative protein modeling, *Electrophoresis 18*, 2714−2723.
29. Delano, W. L. (2002) *The PyMOL molecular graphics program*, DeLano Scientific, San Carlos, CA.
30. Park, H.-W., Boduluri, S. R., Moomaw, J. F., Casey, P. J., and Beese, L. S. (1997) Crystal structure of protein farnesyltransferase at 2.25 Å resolution, *Science 275*, 1800−1804.
31. Turek-Etienne, T. C., Strickland, C. L., and Distefano, M. D. (2003) Biochemical and structural studies with prenyl diphosphate analogues provide insights into isoprenoid recognition by protein farnesyl transferase, *Biochemistry 42*, 3716−3724.
32. Strickland, C. L., Weber, P. C., Windsor, W. T., Wu, Z., Le, H. V., Albanese, M. M., Alvarez, C. S., Cesarz, D., del Rosario, J., Deskus, J., Mallams, A. K., Njoroge, F. G., Piwinski, J. J., Remiszewski, S., Rossman, R. R., Taveras, A. G., Vibulbhan, B., Doll, R. J., Girijavallabhan, V. M., and Ganguly, A. K. (1999) Tricyclic farnesyl protein transferase inhibitors: crystallographic and calorimetric studies of structure−activity relationships, *J. Med. Chem. 42*, 2125−2135.
33. Tobin, D. A., Pickett, J. S., Hartman, H. L., Fierke, C. A., and Penner-Hahn, J. E. (2003) Structural characterization of the zinc site in protein farnesyltransferase, *J. Am. Chem. Soc. 125*, 9962−9969.

34. Ohnuma, S.-i., Hirooka, K., Hemmi, H., Ishida, C., Ohto, C., and Nishino, T. (1996) Conversion of product specificity of archaebacterial geranylgeranyl-diphosphate synthase, *J. Biol. Chem. 271*, 18831−18837.
35. Ohnuma, S.-i., Hirooka, K., Ohto, C., and Nishino, T. (1997) Conversion from archaeal geranylgeranyl diphosphate synthase to farnesyl diphosphate synthase, *J. Biol. Chem. 272*, 5192−5198.
36. Ohnuma, S.-i., Nakazawa, T., Hemmi, H., Hallberg, A.-M., Koyama, T., Ogura, K., and Nishino, T. (1996) Conversion from farnesyl diphosphate synthase to geranylgeranyl diphosphate synthase by random chemical mutagenesis, *J. Biol. Chem. 271*, 10087−10095.

BI060295E